The European Journal of Research and Development

journals.orclever.com/ejrnd

OR CLEVER Science & Research Group

Research Article

Analysis of Dual-Band Plasmonic Nanoantenna with Ultra-Thin Circular Gold Layers in Visible Region

Hayriye Demirtas[1*], Mustafa Turkmen[2,3,4*], Ekin Aslan[5], [*]Erdem Aslan[6*]

[1] Erciyes University, Kayseri, Turkey (0000-0002-1015-0235), unluhayriye3@gmail.com
[2] Erciyes University, Kayseri, Turkey (0000-0002-5257-8256), turkmen@erciyes.edu.tr
[3] Fotonik Technology Co. Inc., Kayseri, Turkey (0000-0002-5257-8256), mt@fotonik.com.tr
[4] Nokta Engineering Co. Inc., Istanbul, Turkey (0000-0002-5257-8256), mt@noktadetectors.com
[5] Kayseri University, Kayseri, Turkey (0000-0003-0933-7796), ekinaslan@kayseri.edu.tr
[6] Erciyes University, Kayseri, Turkey, 0000-0001-6829-9000, aslanerdem@erciyes.edu.tr
[*] Correspondence: turkmen@erciyes.edu.tr

(First received March 12, 2022 and in final form June 02, 2022)

Reference: Demirtas, H., Turkmen, M. ., Aslan, E. ., & Aslan, E. Analysis of Dual-Band Plasmonic Nanoantenna with Ultra-Thin Circular Gold Layers in Visible Region. *The European Journal of Research and Development*, *2*(2), 329–337.

Abstract

Aperture-based plasmonic nanoantenna design with dual-band resonance obtained in the region very close to the green wavelength in the spectrum between 400 nm and 700 nm, which can be used in non-invasive biological sensing applications in the future, is presented. In this circular aperture-based nanoantenna design, the effect of changing the material thickness and dielectric medium parameters on the antenna response is investigated. In the nanoantenna design using a double-layer conductive gold layer, both of thickness values are reduced to 5 nm. It is observed that this thickness value exhibits a very strong transmittance response compared to the thicker gold layer values used in the visible region. In this nanoantenna, which exhibits dual band properties at 508 and 551 nm wavelengths, the strongest transmittance peaks are obtained for 5 nm thickness of gold, 100 nm thickness of magnesium fluoride and the 100 nm radius of the circular aperture. In order to contribute to spectroscopic sensing applications, hot spots locations and near field enhancement distribution maps are also examined.

Keywords: Dual-Band Resonances, Nanoantenna, Plasmonics, Metamaterials

1. Introduction

Detection of pathogenic molecules such as viruses, bacteria, as well as biological molecules such as protein and DNA become the focus of attention after the pandemic. Detection of these molecules is important to diagnose the diseases and for the correct

treatment phase. Molecule detection applications can be carried out by many methods such as PCR and culturing [1-3]. However, existing applications have some disadvantages due to reasons such as labeling, cost, time, and the need for experienced personnel. For this reason, there is a need for functional detection mechanisms that can detect quickly and accurately and do not require expertise. A solution for this problem is the plasmonic nanostructures that can be employed for biosensing applications. As the light reaches to the metal surface, photons interact with free electrons of the metal and create the surface plasmons (SPs) [4,5]. Localized SPs on the surface of metal particles, with their ability to trap light at the subwavelength scale, are the main physical tool of the plasmonics [6]. The SP resonances of metallic nanostructures depend on the refractive index of the surrounding medium [7], the shape and direction of the apertures [8,9], the aperture size, and metal thickness [10-13]. By changing these dimensions and geometric structure, the system frequency can be tuned to the targeted region [14]. Thanks to their unique properties, plasmonic nanoantennas play an important role in the ultrasensitive detection of biological and chemical molecules [15,16].

In this work, a dual-band plasmonic nanoantenna with ultra-thin circular gold layers in visible region (VIS) is proposed. The double gold layer, which is used as the conductive layer, is analyzed as an ultra-thin film. The frequency responses of this circular shaped aperture-based geometry in the VIS range are investigated. The near-field and the far-field analyzes of this structure are carried-out and the electric field distributions are also examined between 400 nm – 700 nm range.

2. Materials and Methods

The aperture-based plasmonic nanoantenna array is numerically analyzed by using Finite Difference Time Domain (FDTD) method. The effects of the dielectric cladding parameters on the transmittance, reflectance, and the electric field distribution are numerically investigated. The proposed structure has a 5 nm thick Au layer on a 100 nm thick silicon nitride (Si_3N_4) substrate with 425 nm x 425 nm unit cell periodicities along the x- and y-axes. 100 nm thick magnesium fluoride (MgF_2) layer is used since MgF_2 has a low refractive index, it is preferred as a dielectric and the separating layer [17]. The refractive index constant of MgF_2 and the dispersion data used for the Au layer are taken from the references [18,19]. After the top layer is coated with 5 nm Au film, circular nano-apertures are formed up to the bottom layer. The structure and dimensions of the nanoantenna are shown in Figure 1.

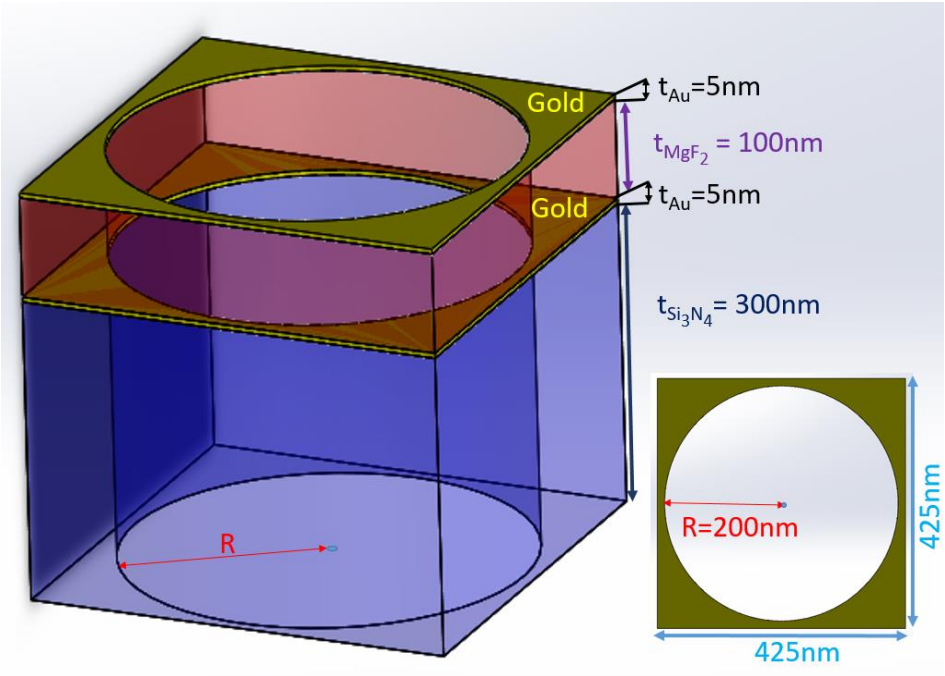

Figure 1. *Design and dimensions of circular nanoaperture-based nanoantenna structure*

The plane wave propagating along the z-axis is used as a source in the simulations. The boundaries along the x and y axis are chosen for periodic conditions, while the z axis is chosen as perfectly matched layers (PML). The minimum mesh step is 5 nm. The nanoantenna response is investigated by increasing the thickness of the layers forming the structure. The change in transmittance response is examined by increasing the R value, which is the radius of the circular aperture, by 50 nm in the range of 50 nm – 150 nm. Similarly, the thickness of the MgF_2 layer is increased by 50 nm in the range of 50 nm - 250 nm, and its effect on the transmittance curve is investigated. The thickness of Au layer, which is the double-layer conductive layer of the antenna, is applied for different values between of thicknesses between 5 and 100 nm. Thus, the VIS region behavior of the nanoantenna is evaluated. The transmittance response with the highest peak value in the analyzes is obtained for the dimensions R = 200 nm, t_{MgF_2} = 100 nm, t_{Au} = 5 nm.

Additionally, transmittance and reflectance responses of the proposed nanoantenna array are investigated via taking the refractive index of the dielectric cladding medium as n = 1.37 and n = 1.42. The results of the electric field distribution are shown using dual monitors for 508 nm and 551 nm wavelengths.

3. Results

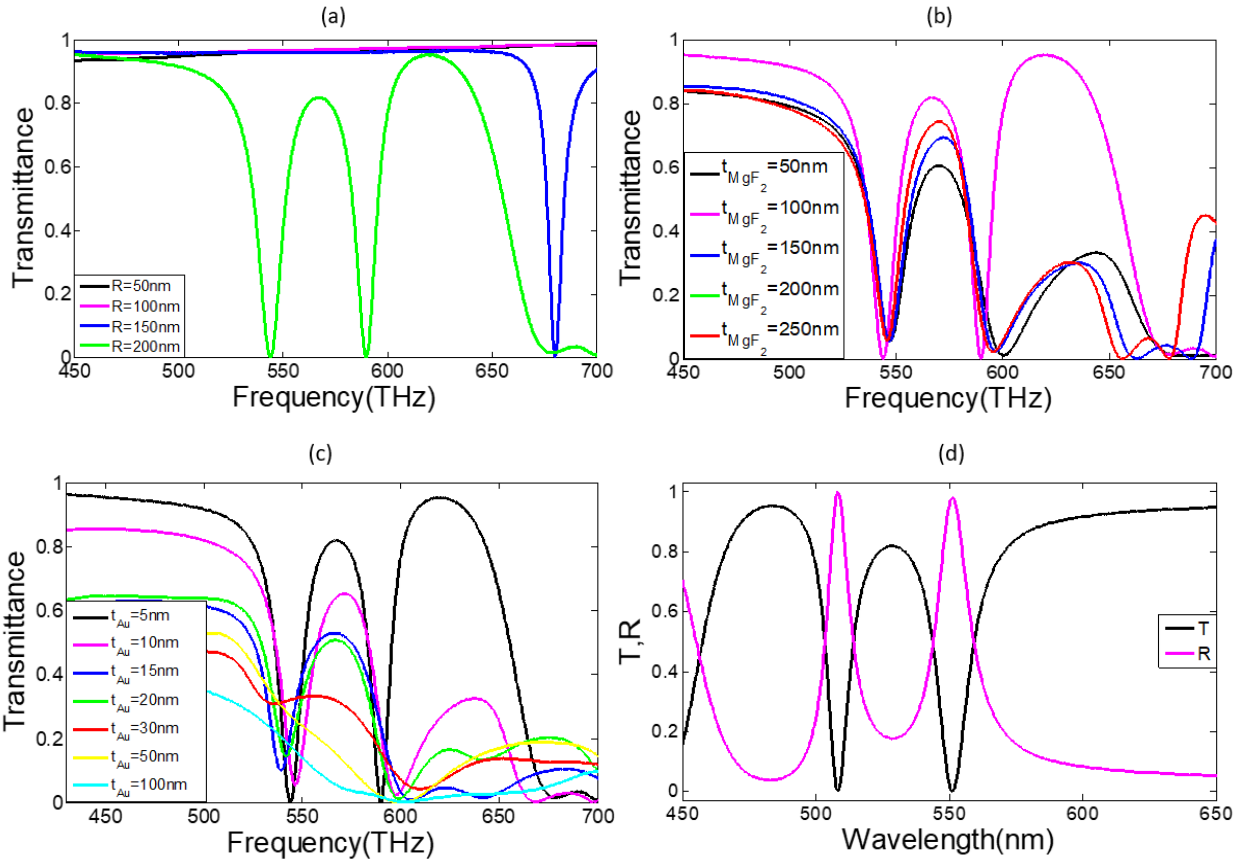

Figure 2. *Effects of thickness changes on transmittance response (a) Transmittance response change with respect to radius change of circular nanoaperture. (b) Transmittance response change according to the thickness change of the MgF_2 layer between 50 nm and 250 nm. (c) Change of transmittance response with change in thickness of bilayer Au layers. (d) The wavelength-dependent variation of the transmittance and reflectance response of the structure designed using the data with the highest peak in thickness analysis, R = 200 nm, t_{MgF_2} = 100 nm, t_{Au} = 5 nm*

The various frequency responses of the antenna, depending on the geometric dimensions of the antenna, the change in Au thickness, and the dielectric cladding parameters, are investigated. With this design, frequency optimization can be achieved in accordance with the molecule desired to be detected, depending on the size associated with dimensions, thickness and dielectric cladding constants. The frequency ranges to which this developed plasmonic, aperture-based, circular cross-section nanoantenna design is sensitive are shown. The R value, which is the radius of the circular aperture, is increased by 50 nm in the range of 50 nm - 150 nm. As a result, it is seen in Figure 2.a that the highest peak value is reached at R = 200 nm. Moreover, it is observed that it reaches a peak value at a wavelength close to the double band feature

and the green wavelength (λ = 550 nm). This resonance value peaked in a region close to the band gap covering biological molecules.

According to the analysis carried out by increasing the MgF_2 layer thickness by 50 nm in the range of 50 nm - 250 nm, it is seen in Figure 2(b) that the transmittance value approached 1 for the MgF_2 thickness value of 100 nm. It is observed that the Au layers, which are the conductive layers of the circular aperture-based nanoantenna, have the highest transmittance value in the VIS region range for t_{Au} = 5 nm, according to the thickness variations. The behavior of Au in the VIS region deteriorated when the Au thickness is increased and its transmittance decreased as shown in Figure 2(c). Considering the optimum data obtained as a result of the simulations, when the layer thicknesses are t_{MgF_2} = 100 nm, t_{Au} = 5 nm and the radius is R = 200 nm, the reflectance and transmittance response of the nanoantenna is shown in Figure 2(d). In the reflectance and transmittance curves of the nanoantenna, two peaks are found at 508 nm and 551 nm wavelengths.

4. Variation of Dielectric Environment Parameters and Electromagnetic Field Distributions

To obtain the dependence of the plasmonic resonances on the cladding medium at the specific resonant frequencies, it is investigated for correspondence between dielectric constant and resonant response [6]. The change of the nanoantenna environment depending on the wavelength of the reanalyzed nanoantenna by taking the refractive index n = 1.37 and n = 1.42 is shown in Figure 3.

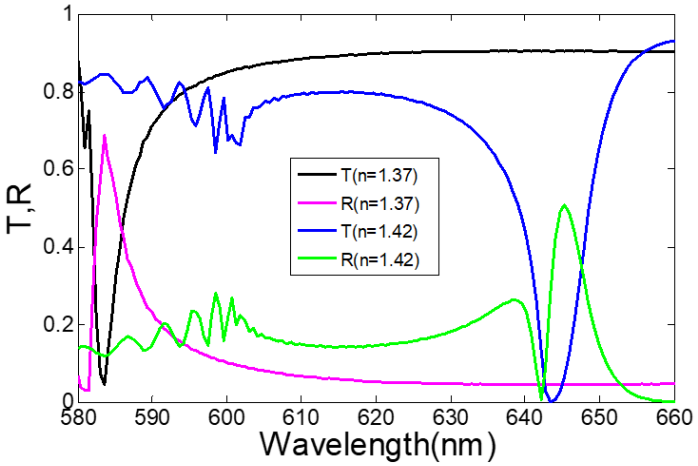

Figure 3. *Transmittance and reflectance spectra for the refractive index values of 1.37 and 1.42. (R = 200 nm, t_{MgF_2} = 100 nm, t_{Au} = 5 nm) according to dielectric cladding parameters of circular nanoaperture*

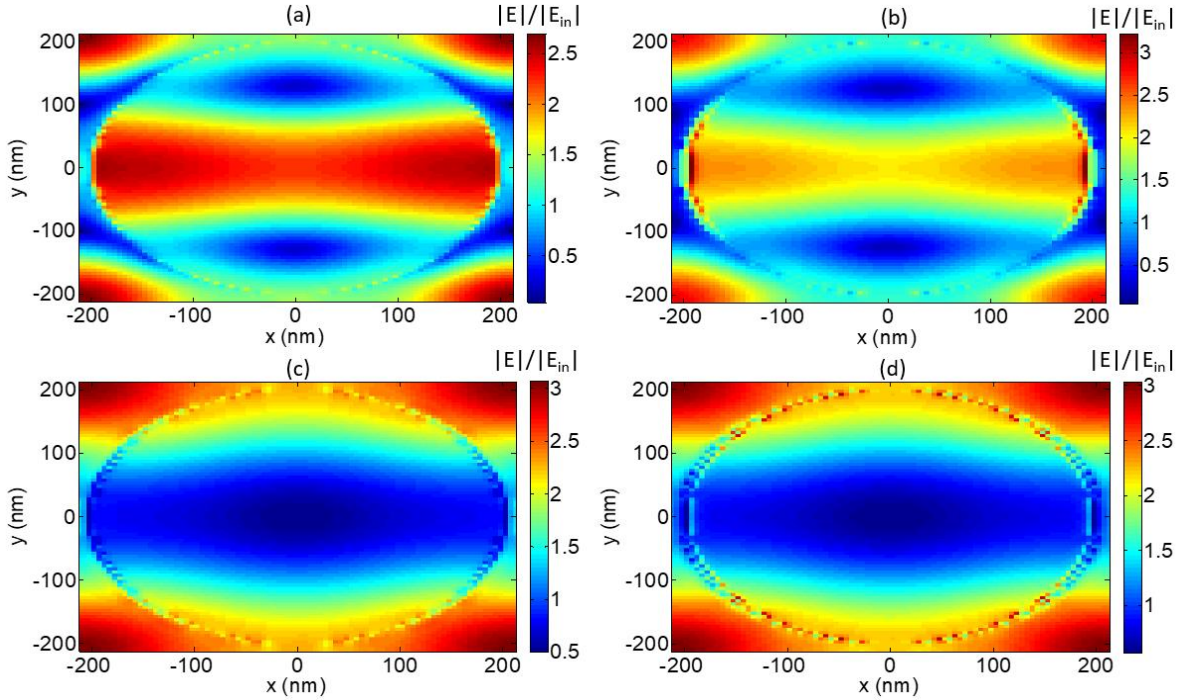

Figure 4. *For λ = 508 nm. (a) Si_3N_4 - Au interlayer monitor (b) Au - MgF_2 first interlayer monitor. (c) MgF_2 - Au second interlayer monitor. (d) Electric field distributions in the Au - air second interlayer monitor*

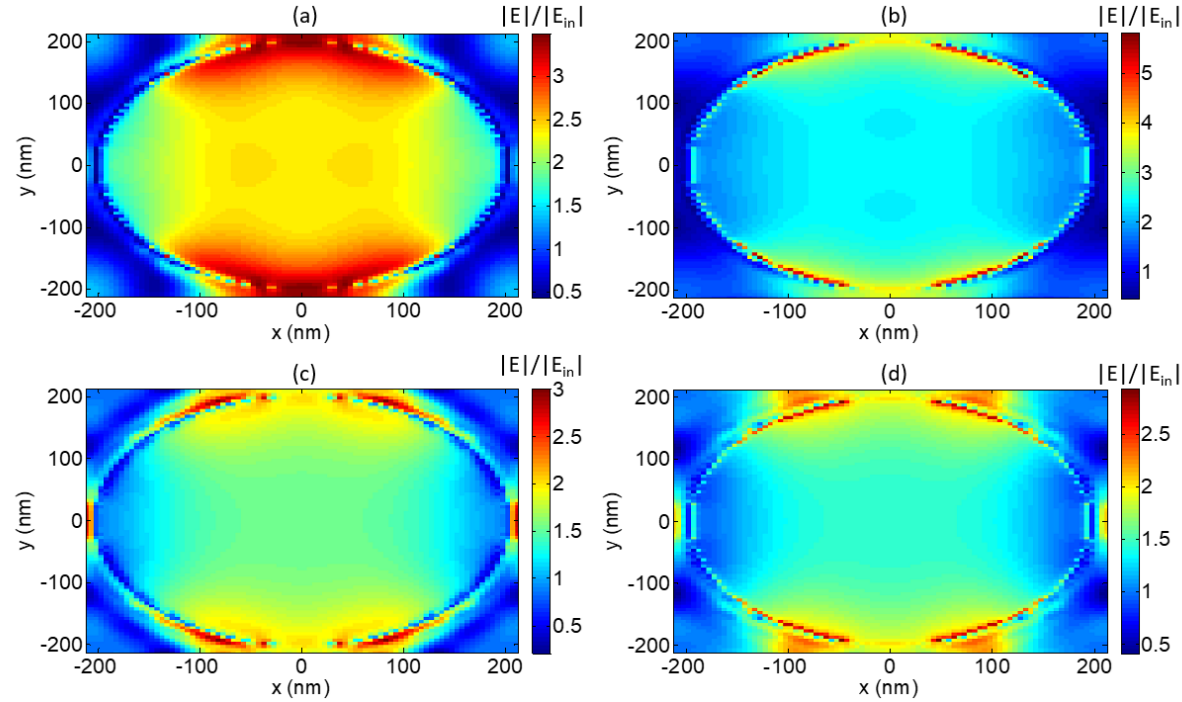

Figure 5. *For λ = 551 nm. (a) Si_3N_4 - Au interlayer monitor (b) Au - MgF_2 first interlayer monitor. (c) MgF_2 - Au second interlayer monitor. (d) Electric field distributions in the Au - air second interlayer monitor*

In spectroscopic sensing applications, the enhancement of the molecular vibrational modes strongly depends on the near-field intensity at the hot-spots locations [6]. The hot-spots amplify the molecular vibrations of biomolecules, making detection efficiently. For this reason, the excess and density of the spots are very important. In this context, electric field intensity distribution graphs are shown in Figure 4 and Figure 5. According to the area distributions, it is seen that the circular section is dense in the edge regions and electric dipole moment induces corresponding hot spot localizations.

5. Discussions and Conclusion

It is shown that the transmittance results of the circular aperture nanoantenna array with a double Au plasmonic layer separated by MgF_2 spacer layer depend on the thickness of the materials used and the dielectric cladding parameters. The most striking change for the results obtained is seen when the Au thickness is analyzed as 5 nm. As far as we know, it is not investigated before in the literature such a small Au layer thickness. Moreover, it is not seen that the response of the nanoantenna in the VIS region in the 400 - 700 nm wavelength range is strengthened with such a small Au thickness. It is possible to adjust the antenna response to the desired frequency by changing the thickness of the layers that make up this aperture-based nanoantenna. With this optimization, it is expected to be effective in biological molecule detection applications. The MgF_2 interlayer inserted between the double Au conductive layer provides the near-field plasmon interaction, which supports the capture of incident light [11]. There are circular aperture nanoantenna designs similar to this study in the literature [20, 21]. While the Au thickness is taken as 100 - 150 nm in other studies, it is reduced to 5 nm in the study. In this way, compared to other studies with a single peak, two sharp and narrow peaks are obtained at 508 and 551 nm wavelengths in this study. In addition, according to the data obtained, results very close to 550 nm, which is the green wavelength of biological molecules, are obtained. This is an advantage for the nanoantenna designed in this way to be used in biological sensing applications.

6. Acknowledgement

Hayriye Demirtaş acknowledge the scholarship grant supported by The Council of Higher Education of Turkey (Program Code: YOK 100/2000 PhD Scholarship).

References

1. Gerrits, M. M., van Vliet, A. H., Kuipers, E. J., & Kusters, J. G. (2006). “Helicobacter pylori and antimicrobial resistance: molecular mechanisms and clinical implications.”, The Lancet infectious diseases, 6(11), 699-709.

2. Kawai, S., Arai, K., Lin, Y., Nishiyama, T., Sasakabe, T., Wang, C. & Kikuchi, S. (2019). Comparison of the detection of Helicobacter pylori infection by commercially available serological testing kits and the 13C-urea breath test. Journal of Infection and Chemotherapy, 25(10), 769-773.
3. Seddon, A. B. (2013). Mid-infrared (IR)–A hot topic: The potential for using mid-IR light for non-invasive early detection of skin cancer in vivo. physica status solidi (b), 250(5), 1020-1027.
4. Cao, J., Sun, T., & Grattan, K. T. (2014). Gold nanorod-based localized surface plasmon resonance biosensors: A review. Sensors and actuators B: Chemical, 195, 332-351.
5. Barnes, W. L., Dereux, A., & Ebbesen, T. W. (2003). Surface plasmon subwavelength optics. nature, 424(6950), 824-830.
6. Aslan, E., Aslan, E., Turkmen, M., & Saracoglu, O. G. (2017). Metamaterial plasmonic absorber for reducing the spectral shift between near-and far-field responses in surface-enhanced spectroscopy applications. Sensors and Actuators A: Physical, 267, 60-69.
7. Chen, H., Ran, L., Huangfu, J., Zhang, X., Chen, K., Grzegorczyk, T. M., & Kong, J. A. (2004). Metamaterial exhibiting left-handed properties over multiple frequency bands. Journal of Applied Physics, 96(9), 5338-5340.
8. Thio, T., Ghaemi, H. F., Lezec, H. J., Wolff, P. A., & Ebbesen, T. W. (1999). Surface-plasmon-enhanced transmission through hole arrays in Cr films. JOSA B, 16(10), 1743-1748.
9. Azad, A. K., Zhao, Y., & Zhang, W. (2005). Transmission properties of terahertz pulses through an ultrathin subwavelength silicon hole array. Applied Physics Letters, 86(14), 141102.
10. Degiron, A., Lezec, H. J., Barnes, W. L., & Ebbesen, T. W. (2002). Effects of hole depth on enhanced light transmission through subwavelength hole arrays. Applied Physics Letters, 81(23), 4327-4329.
11. Aslan, E., Aslan, E., Saracoglu, O. G., & Turkmen, M. (2019). An effective triple-band enhanced-infrared-absorption detection by honeycomb-shaped metamaterial-plasmonic absorber. Sensors and Actuators A: Physical, 288, 149-155.
12. Aslan, E., Kaya, S., Aslan, E., Korkmaz, S., Saracoglu, O. G., & Turkmen, M. (2017). Polarization insensitive plasmonic perfect absorber with coupled antisymmetric nanorod array. Sensors and Actuators B: Chemical, 243, 617-625.
13. Korkmaz, S., Turkmen, M., & Aksu, S. (2020). Mid-infrared narrow band plasmonic perfect absorber for vibrational spectroscopy. Sensors and Actuators A: Physical, 301, 111757.
14. Cetin, A. E., Kaya, S., Mertiri, A., Aslan, E., Erramilli, S., Altug, H., & Turkmen, M. (2015). Dual-band plasmonic resonator based on Jerusalem cross-shaped nanoapertures. Photonics and Nanostructures-Fundamentals and Applications, 15, 73-80.
15. Schuller, J. A. (2010). Edward Barnard, Wenshan Cai, Young Chul Jun, Justin White, Mark L. Brongersma, Invited Review for Nature Materials, 9, 193-204. Anker, J. N., Hall, W. P., Lyandres, O., Shah, N. C., & Zhao, J. Van duyne RP (2008). Biosensing with plasmonic nanosensors. Nat. Mater, 7, 442-453.

16. Stewart, M. E., Anderton, C. R., Thompson, L. B., Maria, J., Gray, S. K., Rogers, J. A., & Nuzzo, R. G. (2008). Nanostructured plasmonic sensors. Chemical reviews, 108(2), 494-521.
17. Aslan, E., Aslan, E., Turkmen, M., & Saracoglu, O. G. (2017). Experimental and numerical characterization of a mid-infrared plasmonic perfect absorber for dual-band enhanced vibrational spectroscopy. Optical Materials, 73, 213-222.
18. Chen, K., Adato, R., & Altug, H. (2012). Dual-band perfect absorber for multispectral plasmon-enhanced infrared spectroscopy. ACS nano, 6(9), 7998-8006.
19. E.D. Palik, Handbook of Optical Constants of Solids, vol. III, Academic Press,1998.
20. Cetin, A. E., & Topkaya, S. N. (2019). Plasmonic diffraction field pattern imaging could resolve ultrasensitive bioinformation. ACS Photonics, 6(11), 2626-2635.
21. Gopalan, K. K., Paulillo, B., Mackenzie, D. M., Rodrigo, D., Bareza, N., Whelan, P. R., ... & Pruneri, V. (2018). Scalable and tunable periodic graphene nanohole arrays for mid-infrared plasmonics. Nano letters, 18(9), 5913-5918.